DECOUPLING AND OBSERVATION THEORY APPLIED TO

CONTROL OF A LONG FLEXIBLE BEAM

IN ORBIT

Harold A. Hamer
NASA Langley Research Center
Hampton, Virginia

INTRODUCTION

Decoupling theory is a convenient tool for devising control laws for structures with a large number of state variables because it allows independent control of each state. Complete decoupled control requires that the number of control actuators equal the number of modes in the system, which is a basic limitation in applying decoupling theory to the control of large space structures. Complete decoupled control is usually not achievable in practical application because a large space structure may have an infinite number of flexible modes; hence, procedures must be developed which maintain control of the structure with a small number of control actuators. Reduced-order systems must be utilized wherein only a few modes are included in the math model of the structure when calculating the gains for the feedback control law. In addition, some of the modes in the math model itself may be exempt from the control law if the number of actuators selected is less then the number of modeled modes. In both cases the control system must be designed to avoid serious problems associated with observation and control spillover effects caused by residual modes, which could result in poor performance or an unstable system.

The present analysis presents techniques which use decoupling theory and state-variable feedback to control the pitch attitude and the flexible-mode amplitudes of a long, thin beam. An observer based on the steady state Kalman filter has been incorporated into the control-design procedure in order to estimate the values of the modal-state variables required for the feedback control law.

EQUATIONS OF MOTION

Figure 1 shows the linearized equations of motion used for the decoupled-control analysis of a 450-m long, thin, flexible beam in low Earth orbit. The equations are in modal form. The first equation represents the rigid-body (pitch) mode and includes the gravity-gradient effect, where ω_c is the orbital frequency. In the second equation n represents the number of flexible modes included in the math model, plus the residual modes. The damping term $2 \zeta \omega \dot{A}$ is included inasmuch as the residual modes require a small amount of damping for stability. The objective is to design a control system which provides independent control for each of the decoupled variables.

$$\frac{d^2\theta}{dt^2} + 3\,\omega_c^2\,\theta = \frac{T_p}{J}$$

$$\frac{d^2 A_n}{dt^2} + 2\,\zeta_n\,\omega_n\,\frac{dA_n}{dt} + \omega_n^2\,A_n = \frac{E_m}{M_n}$$

$$n = 1,\ 2,\ 3,\ \ldots$$

Figure 1

BASIC EQUATIONS

Figure 2 shows the basic equations used in the decoupled-control design. The equations are in state-vector form where the states x are the modal amplitudes and rates and include the residual modes. In the decoupling control law, u, the quantity v is the input command vector. The matrices F and G are the feedback and feedforward gains, respectively, which are calculated by the decoupling procedure. The estimator equation calculates the estimates of the modeled states $\hat{x}$ which are required by the control law. (The primes indicate modeled modes only.) The estimator utilizes the observation equation y and Kalman gains K which are precomputed by the steady state Kalman filter. The observation matrix senses attitude at two locations on the beam, where the ϕ values are the corresponding slopes of the mode shapes.

SYSTEM:

$$\dot{x} = Ax + Bu + v$$

$$u = F\hat{x} + Gv$$

$$y = Cx + w$$

ESTIMATOR:

$$\dot{\hat{x}} = A'\hat{x} + B'u + K(y - C'\hat{x})$$

$$= (A' - KC')\hat{x} + KCx + B'u$$

OBSERVATION MATRIX:

$$C = \begin{bmatrix} 1 & \phi_1 & \phi_2 & \phi_3 & - - - - & \phi_n & 0 & 0 & 0 & 0 & - - - - & 0 \\ 1 & \phi_1'' & \phi_2'' & \phi_3'' & - - - - & \phi_n'' & 0 & 0 & 0 & 0 & - - - - & 0 \end{bmatrix}$$

Figure 2

COMPOSITE EQUATIONS

Figure 3 shows the basic equations in composite form as a 20th order system. These equations are used to produce simulated time histories of system responses for various control input commands. The upper set of equations represents the system equations and includes four modeled modes and two residual modes. The lower set represents the estimator equations, which incorporate estimates only of the modeled modes. It is apparent that the control and observation spillover effects are caused by the matrices B_{12x2} and C_{2x12}.

In the present analysis two torque actuators are used; each is one-sixth the distance from the end of the beam. One attitude sensor (e.g., star tracker) is at an actuator location, the other at one-third the distance from the end of the beam. Analyses were also performed by (1) replacing the latter sensor with a rate sensor, and (2) by moving this attitude sensor to the location of the other actuator; in both cases, however, overall performance was not as good as for the original setup.

2 Control Actuators
2 Attitude Sensors
4 Controlled Modes
2 Residual Modes

$$
\begin{pmatrix} \dot{x} \\ \dot{\hat{x}} \end{pmatrix} = \left[\begin{array}{c|c} A_{12x12} & B_{12x2}\,F_{2x8} \\ \hline K_{8x2}C_{2x12} & A'_{8x8} - K_{8x2}C'_{2x8} + B'_{8x2}F_{2x8} \end{array} \right] \begin{pmatrix} x \\ \hat{x} \end{pmatrix} + \left[\begin{array}{cc} B_{12x2} & G_{2x2} \\ \hline B'_{8x2} & G_{2x2} \end{array} \right] \begin{pmatrix} v \end{pmatrix}
$$

Figure 3

DYNAMIC CHARACTERISTICS

The dynamics of the system are shown in figure 4. The natural (open loop) frequencies and damping ratios are given in the second column. The value of 0.001 for ω_θ is the orbital angular velocity (orbital frequency). Small values of damping were assumed for the flexible modes, starting at a low value of 0.005 and increasing each successive mode by 10 percent. The fourth and fifth modes are taken as the residual modes. Some damping is required in these modes to avoid producing a system with constant oscillatory responses.

The last two columns show values selected for the closed-loop dynamics for two decoupled control cases. In the FAST PITCH case the commanded pitch attitude is reached in about 40 seconds; in the SLOW PITCH case about 2 minutes are required. In the first case, the two actuators are used to decouple the pitch attitude and first flexible mode. The symmetric arrangement of the actuators produces an interaction between all four modeled modes such that a full-order F matrix is achieved; i.e., feedback control is available for all 4 modes in the math model. This condition exists only because the absolute values of the control-influence coefficients are the same in both columns of the B matrix. For other control arrangements, techniques have been developed in which the control-influence coefficients and/or the feedback gains are adjusted to produce simplified procedures for achieving overall control of the system. The current analysis also included model errors of up to ± 15 percent in the control-influence matrix, with no apparent detrimental effect on the overall system performance.

In the SLOW PITCH case, the same two actuator locations were employed; however, the control-influence coefficients were slightly changed so that the decoupling control law provided control for two modes only. In this case it was necessary to perform two separate decoupling calculations: (1) the pitch and first flexible modes were decoupled, and (2) the second and third flexible modes were decoupled. The feedback gains obtained from both calculations were then combined to provide control for all four modeled modes.

DYNAMIC CHARACTERISTICS

	NATURAL	DECOUPLED	
		FAST-PITCH RESPONSE	SLOW-PITCH RESPONSE
ω_θ, R/S	.001	.07677	.0302
ω_1	.4275	.70	1.1
ω_2	1.172	2.084	1.1635
ω_3	2.297	3.063	2.091
ω_4	3.797		
ω_5	5.6716		
ζ_θ	0	.736	.70
ζ_1	.005	.2185	.3354
ζ_2	.0055	.863	.2013
ζ_3	.00605	.225	.2344
ζ_4	.00665		
ζ_5	.00732		

Figure 4

CLOSED-LOOP EIGENVALUES

     The symbols in figure 5 depict the eigenvalues of the closed-loop system,
assuming perfect knowledge of the state variables. Also shown are the loci of
closed-loop eigenvalues for the observer as the Kalman gains are increased.
The observer (based on the steady-state Kalman filter) was designed to have a
certain stability margin. This was attained by adding a positive scalar term
to the diagonal elements of the system matrix A'. The gains were changed by
varying this scalar. (The A matrix in the composite equations shown in figure 3,
of course, is not altered.) In calculating the Kalman gains, the objective is
to produce an observer whose response is faster than that of the closed-loop
system with perfect knowledge of the state vector (eigenvalue real parts more
negative than those of the closed-loop system). As shown in figure 5, there is
no problem in meeting this condition for the filter eigenvalue corresponding
to the pitch mode. (Hence, estimates of the pitch attitude should be very
accurate.) However, for the flexible modes, large Kalman gains are required to
drive the eigenvalues past the corresponding closed-loop values. In fact, it was
found that Kalman gains which produced eigenvalues with real parts less than
about -0.1 resulted in poor performance; i.e., excessive control forces and/or
excessive overshoot in the flexible-mode response. An example of this is shown
in a subsequent figure.

Figure 5

16
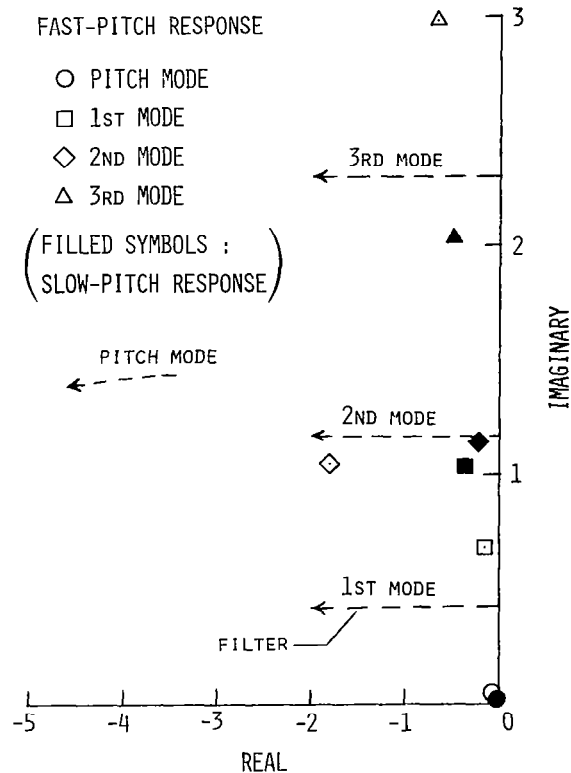
ZERO COMMAND-FAST PITCH

Figure 6 is an example of an instantaneous zero command (FAST PITCH case) to null arbitrary initial disturbances of -0.01 in pitch and 0.015, -0.005, and -0.02 in the first, second, and third flexible modes, respectively, and 0.01 in the residual modes (4th and 5th flexible modes). The Kalman gains used to determine the estimates of the modal variables (shown in 2nd column of time histories) correspond to real eigenvalues = -0.1, as previously discussed. It is assumed that instantaneous control torques T_1 and T_2 are available at time = 0, with initial estimates of 90 percent in pitch attitude and 80 percent in the three modeled flexible mode amplitudes; that is, the control actuators are not turned on until these estimates are established by the observer. Analysis has shown that without the effect of the controls, these estimates are achieved in about 100 seconds. The values of initial disturbances and initial estimates quoted here are used for all figures which follow, except where noted. All figures except figure 13 pertain to the FAST PITCH case.

As shown in figure 6, the four modeled mode responses (first column of time histories) are nulled after about 40 seconds. As for the residual modes, there is some effect on A_5 during the first few seconds; however, responses in both modes gradually die out due to natural damping. It should be noted that, with the controls operating, the observer obtains good estimates of the first three modes, but fails in estimating A_3 due to observation spillover caused by the residual modes. Attempts to improve this estimate by varying the Kalman filter gains are shown in the next two figures.

17
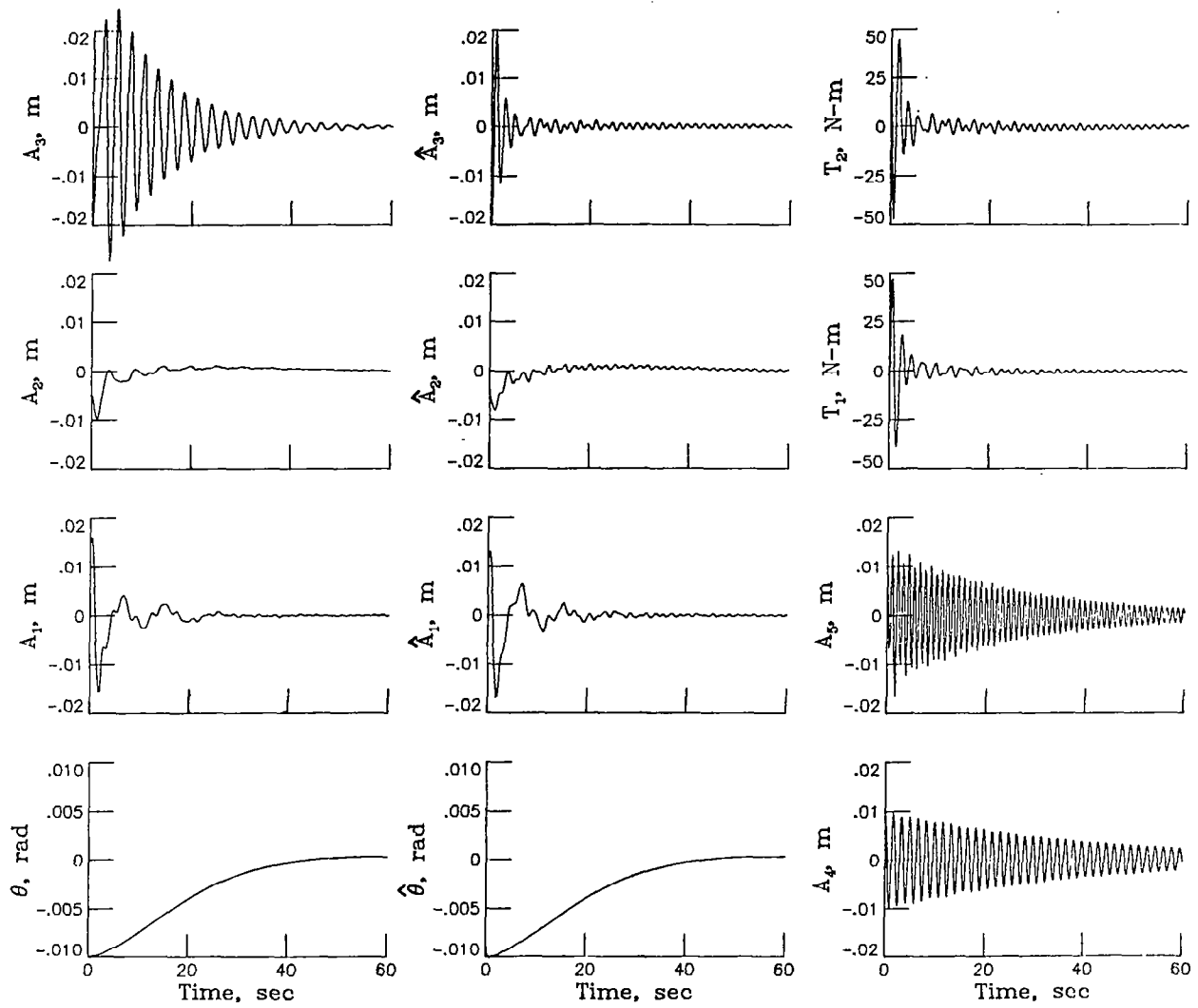
Figure 6

FILTER GAINS REDUCED

For the zero command in figure 7 the Kalman gains were reduced so that the real eigenvalues, corresponding to the flexible modes, were close to zero. This resulted in slowly damped oscillations in the three modeled flexible modes due to poor estimates in all these modes.
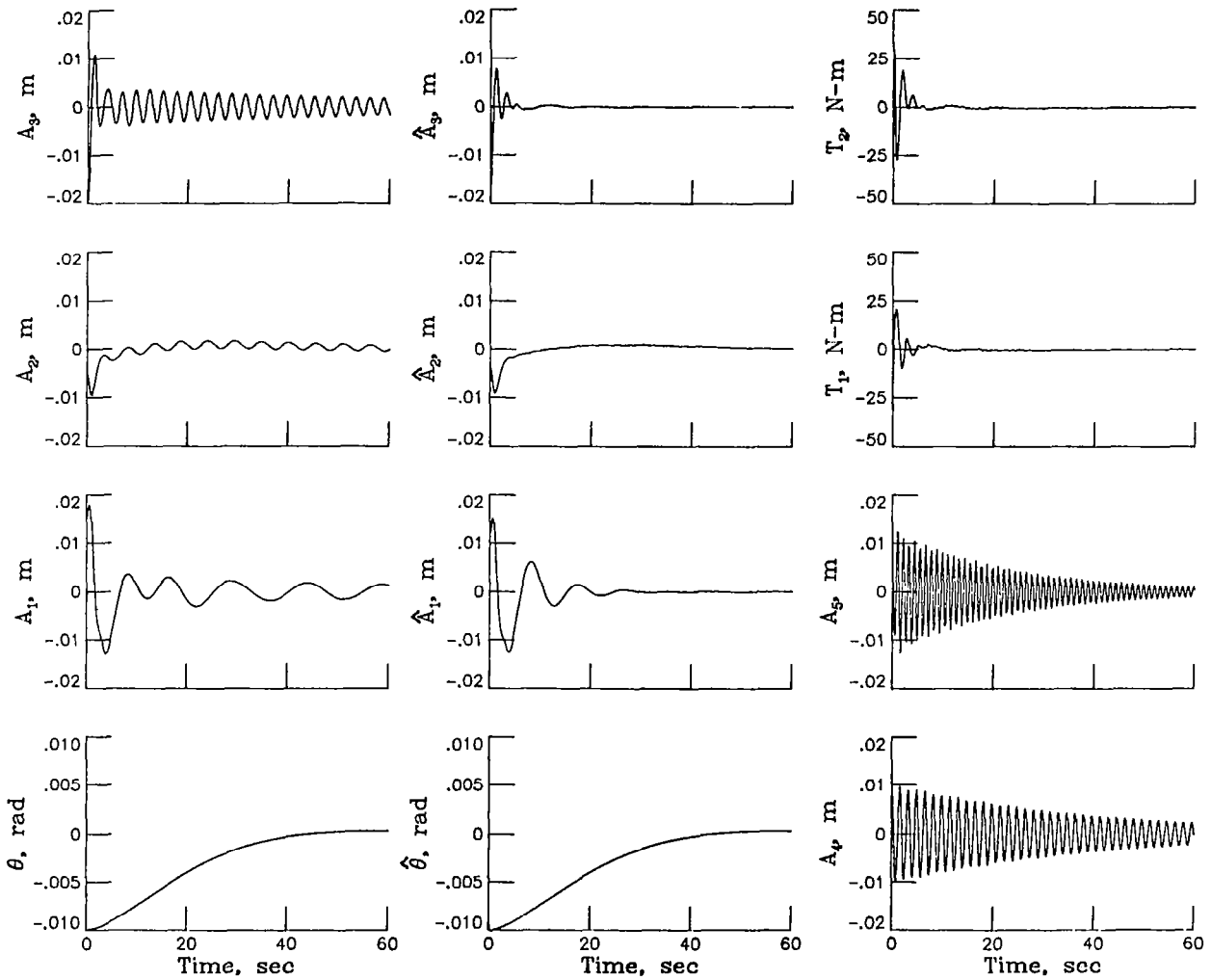

Figure 7

FILTER GAINS INCREASED

The Kalman gains were increased for the zero command case in figure 8 so that the real eigenvalues, corresponding to the flexible modes, were approximately -0.2. Here again, estimates were poor in A_2 and A_3. More notable is the poor performance as exemplified by the increased control torques and the peak overshoots in the flexible mode responses, which far exceeded the initial disturbances. Large control spillover effect is also evident in the residual A_5. Attempts were made to improve the performance for this case, as shown in the next two figures.
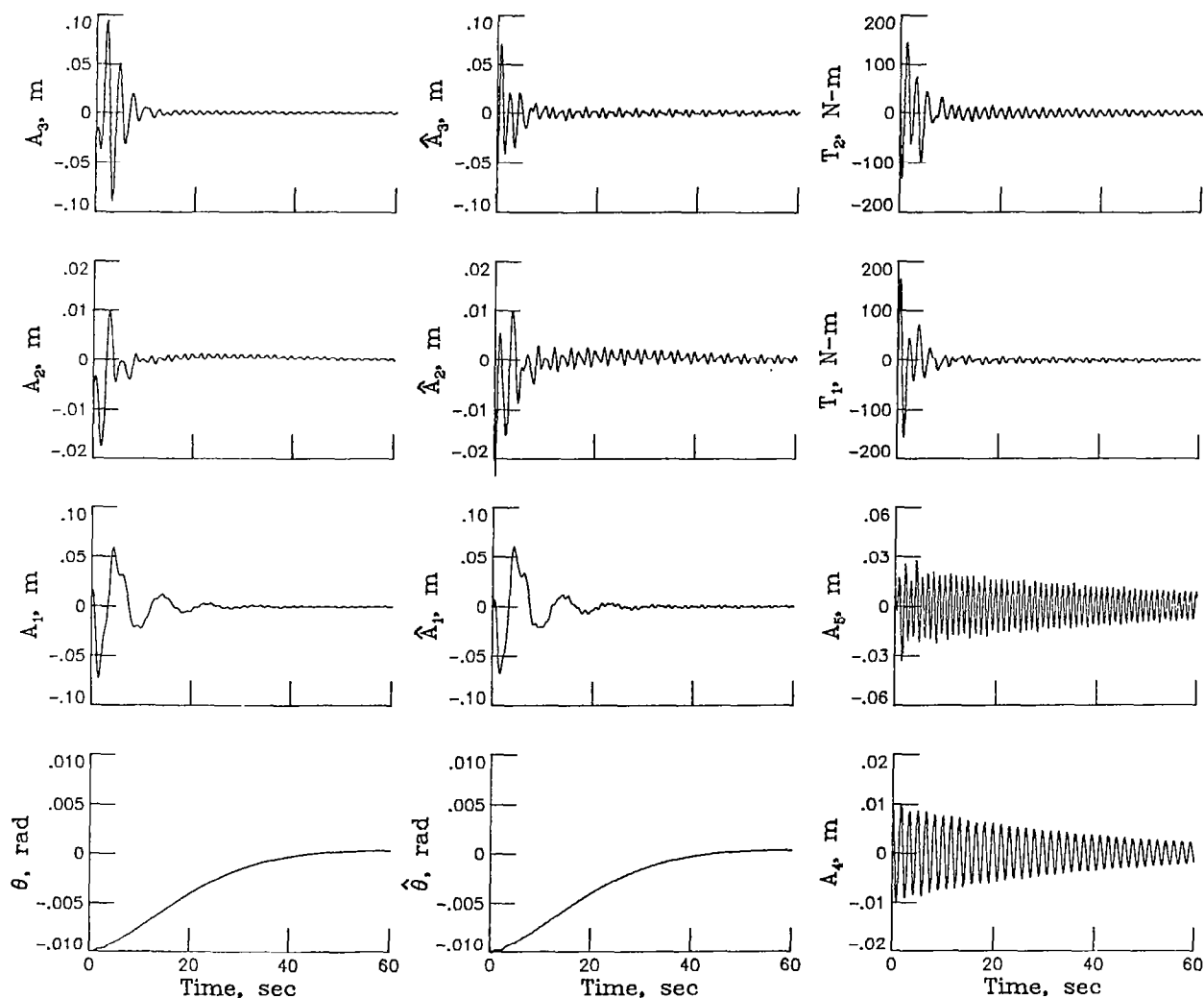
Figure 8

FEEDBACK GAINS ADJUSTED

Figure 9 is similar to figure 8, except the decoupling feedback gain matrix was changed by deleting the gains for the three flexible-mode amplitude displacements. Hence, the control system included feedback gains only for the pitch attitude and rate and the three flexible-mode amplitude rates. As shown by the lower control torques and peak responses, some improvement in performance was accomplished. Also, note the large reduction in the A_5 residual response. The system performance, however, is still unacceptable; the following figure shows a further attempt to improve this performance.
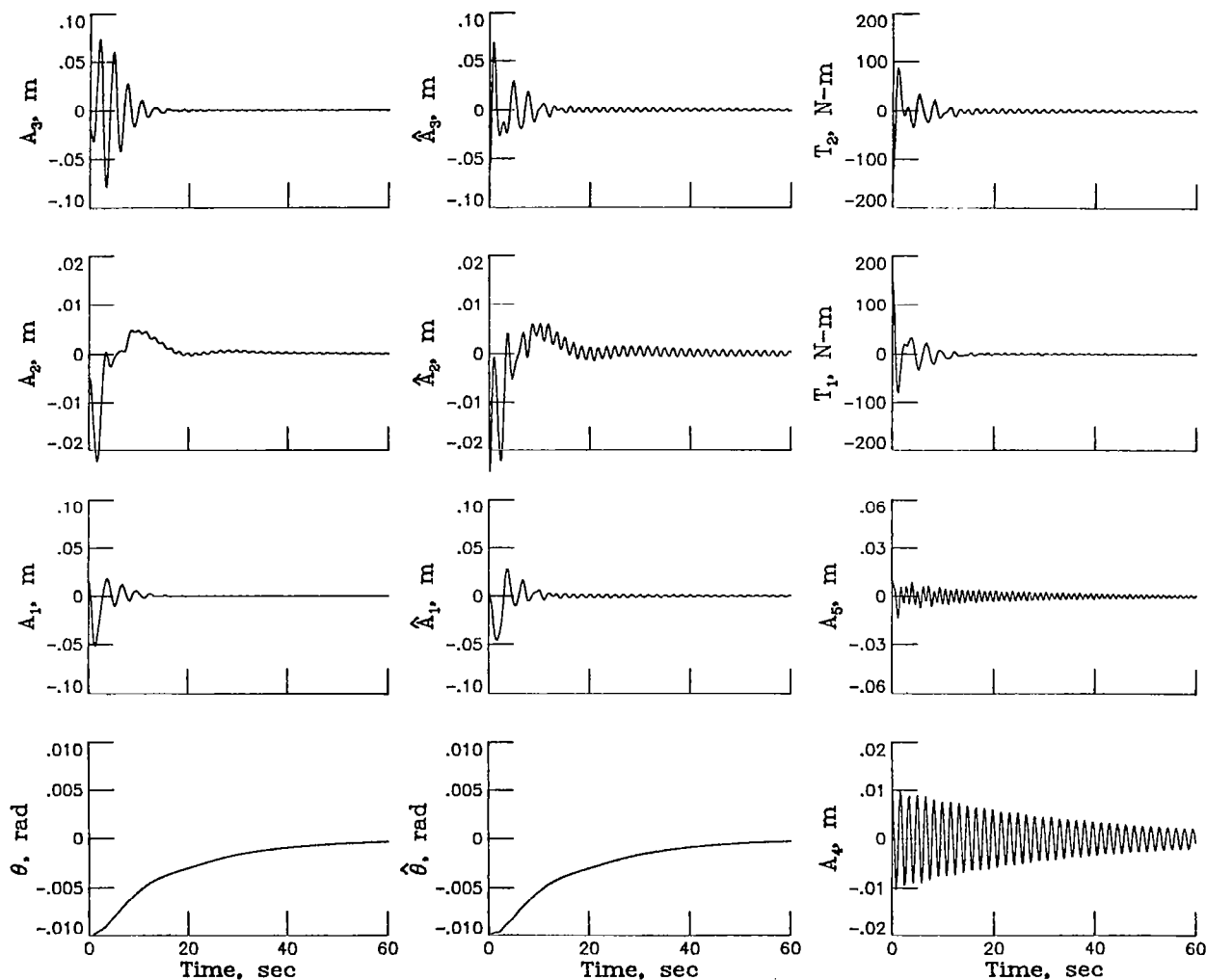
Figure 9

For figure 10, in addition to the feedback gain adjustment, a first order lag (time constant = 5 sec) was included in the control system. This condition more closely resembles practical operational procedures because some lag will always be present in a control system. The results show further improvement in performance (especially in control requirements); however, it appears that the Kalman gains must be reduced for acceptable response in the flexible modes.
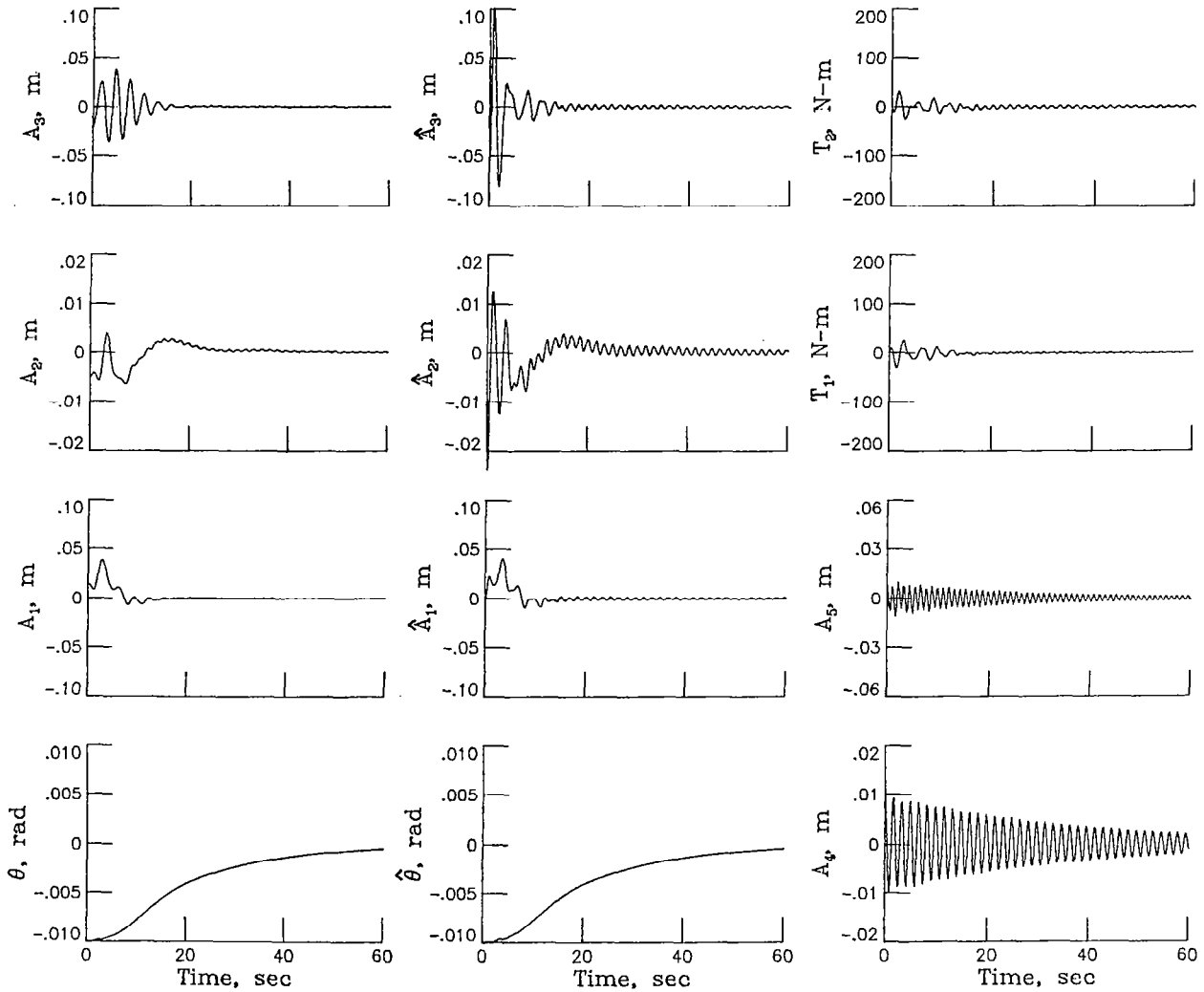
Figure 10

NO PITCH DISTURBANCE

Figure 11 shows a zero command case similar to that of figure 6, except with no initial pitch disturbance. Comparison of the two figures shows the large effect of pitch disturbance on nulling the system. With no pitch to consider (and consequently no error in the initial estimate in pitch), figure 11 shows considerably lower control torques and a much better response in the third flexible mode.
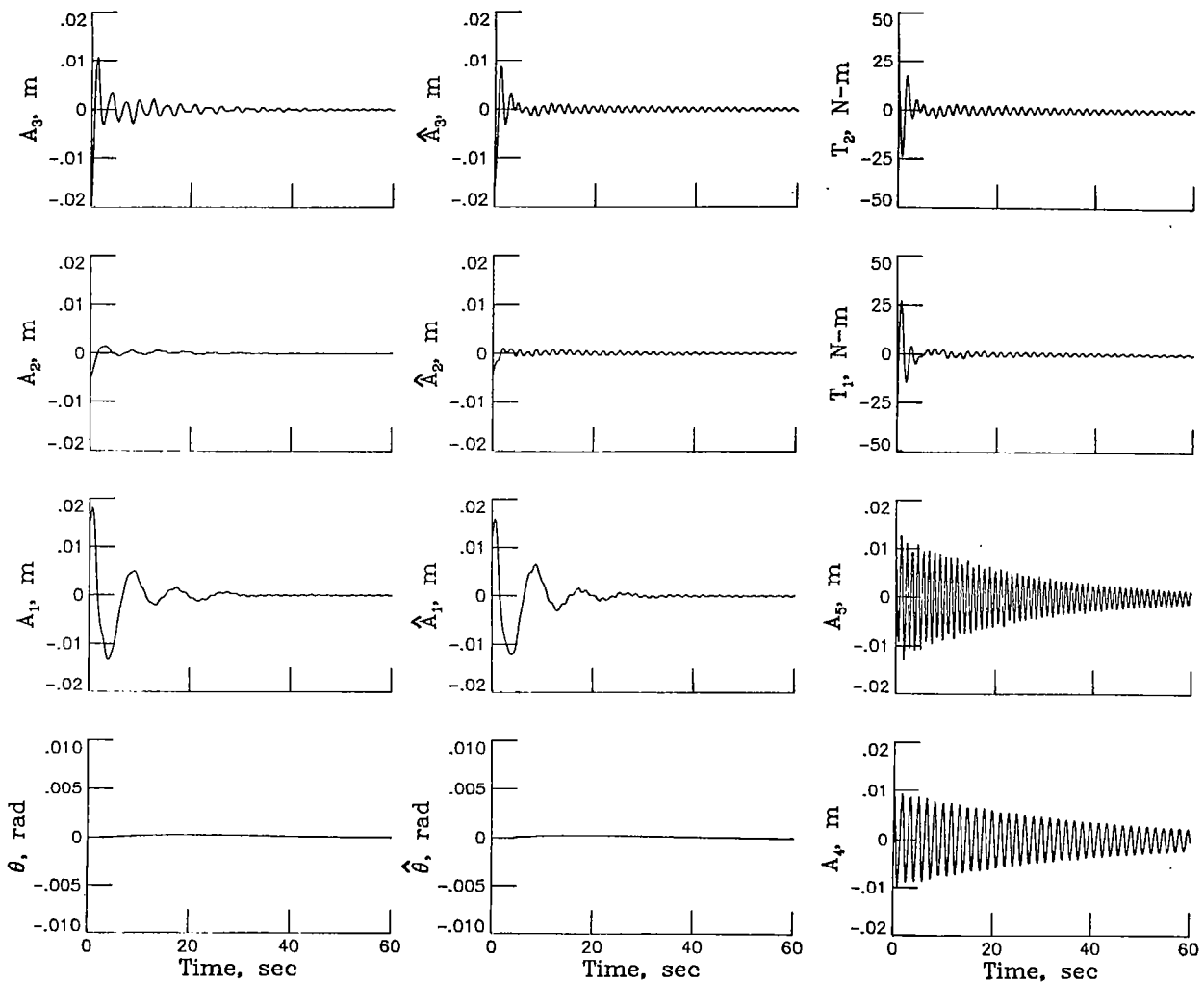
Figure 11

Figure 12 is similar to figure 6, except there are no initial disturbances in the residual modes. Comparison of the two figures shows that the responses in the modeled modes are not materially affected by the motions of the residual modes. Also, the control requirements are about the same in both cases, except for the small lingering oscillations in figure 6.
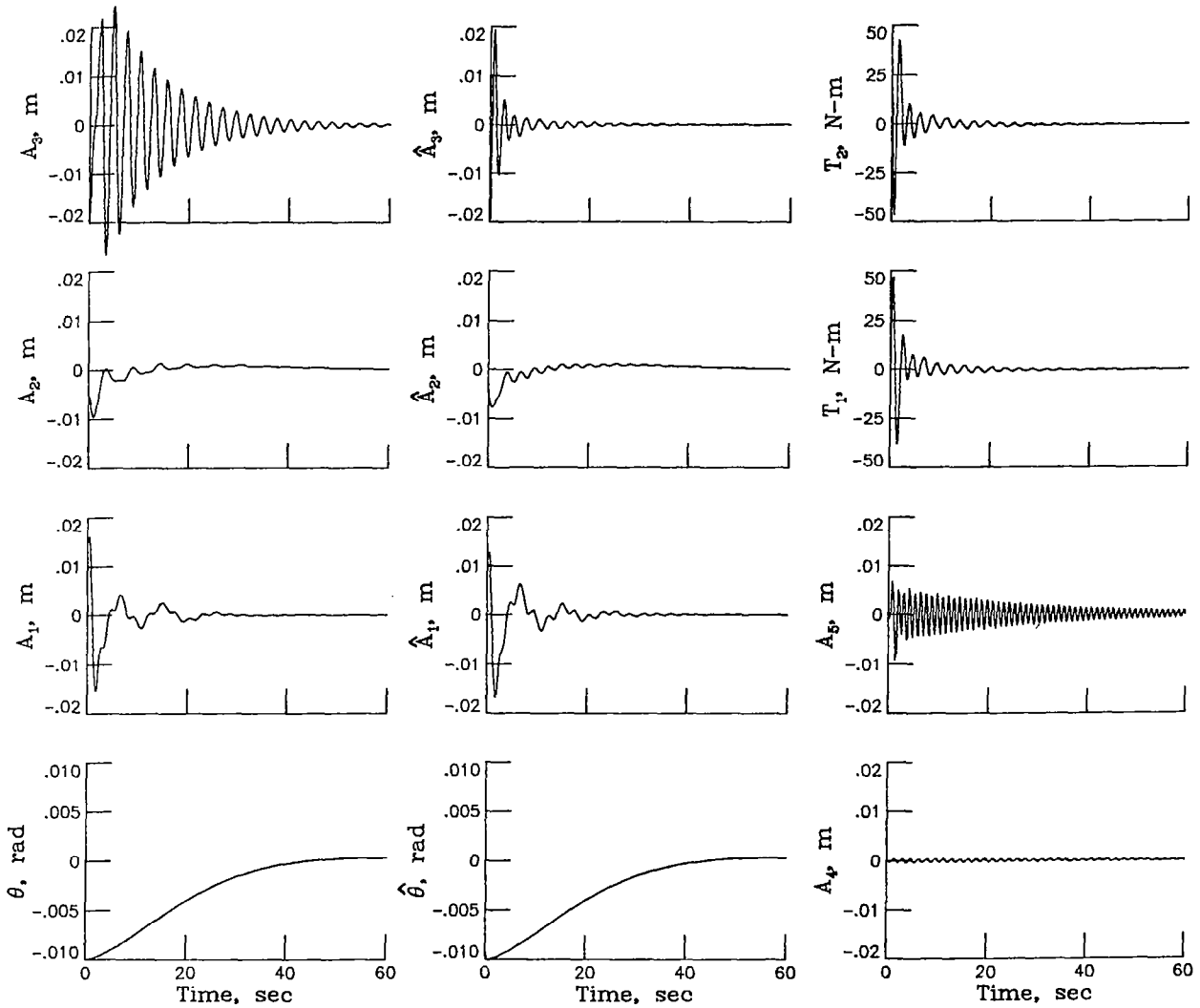
Figure 12

Figure 13 is an example of a zero command for the SLOW PITCH case. The results are similar to the FAST PITCH case (figure 6). Although not shown, about two minutes are required to null the pitch attitude. Also, the maximum control torque is reduced by about one-half, as are the response amplitudes in the residual A_5.

Figure 13

25
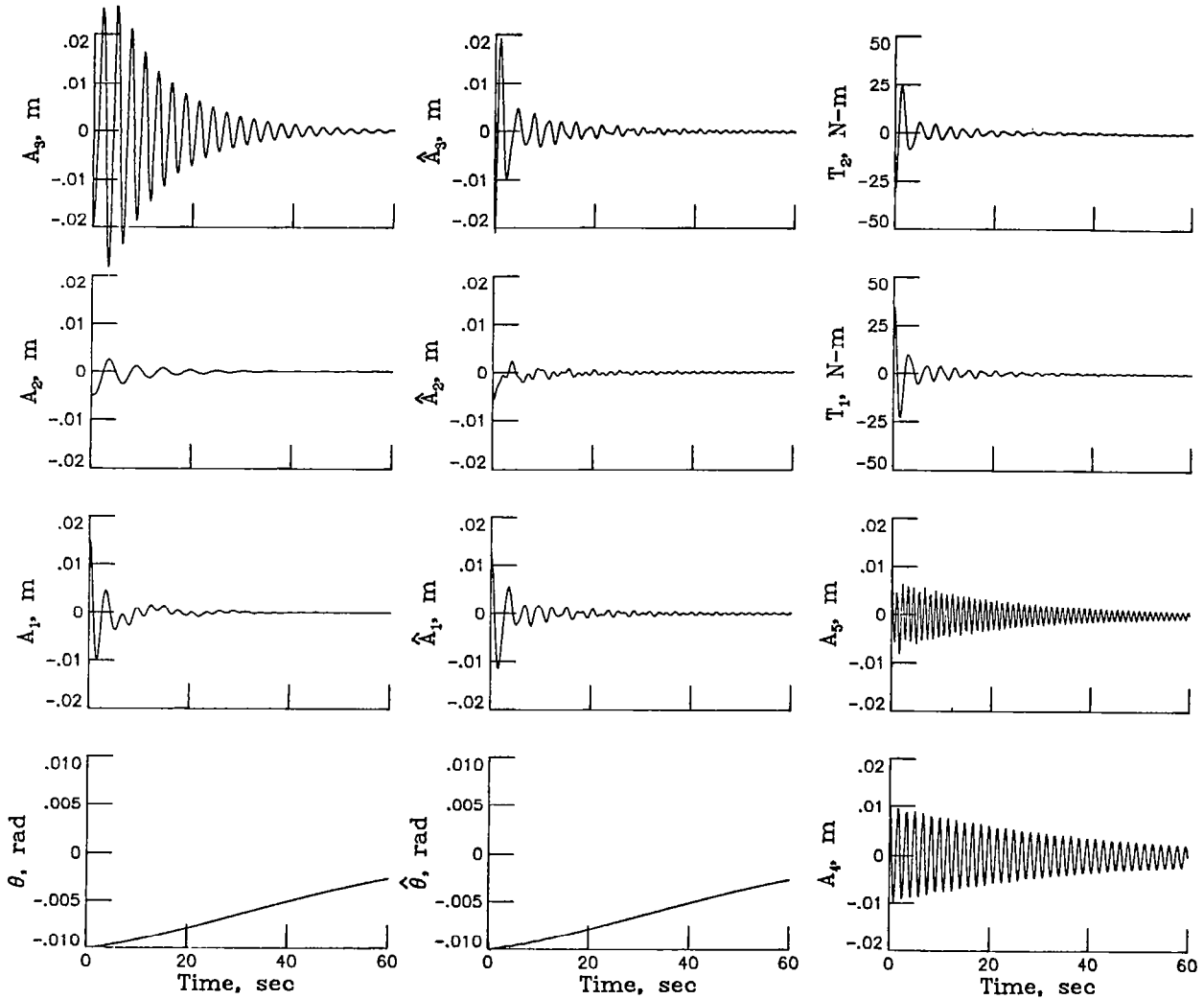
ONE CONTROL INOPERATIVE

Figure 14 is an example of a zero command (FAST PITCH case) where one of
the control actuators is considered to be inoperative. The feedback gains for
the remaining actuator were not altered. The time histories show adequate
responses in nulling the system. In contrast to the two-actuator case (figure 6),
θ and A_1 require about three times as much time to null (Note expanded time
scale).
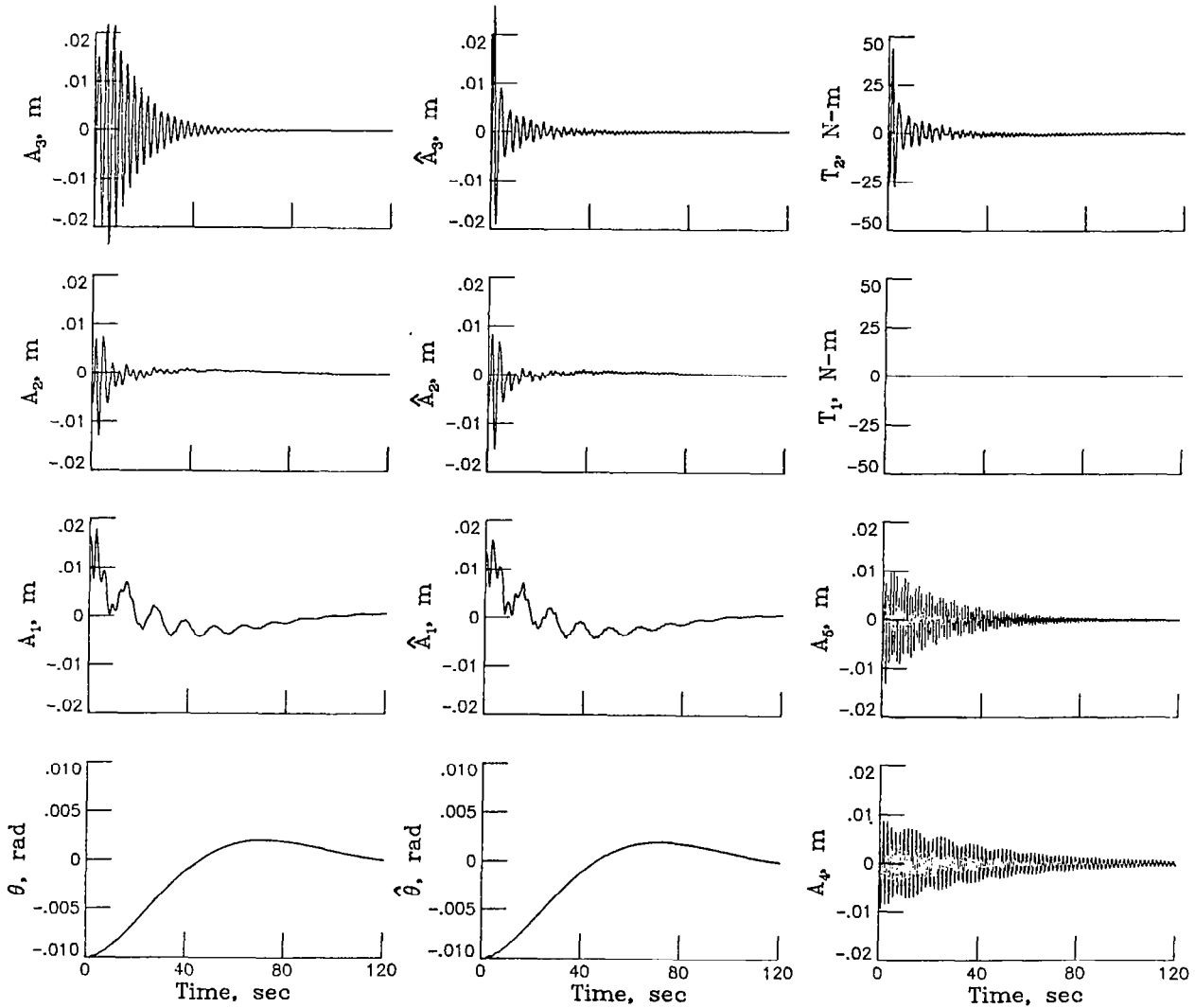
Figure 14

Figure 15 illustrates the same case as the previous figure, except that the decoupling feedback gains were changed in the same manner as in the case of figure 9 and a first-order lag (tau = 5 sec) was included in the control system. Comparison with figure 14 shows better response characteristics for θ and A_1, as well as a large reduction in control requirements. Also, note that the observer obtains good estimates of A_3 after about 30 seconds.
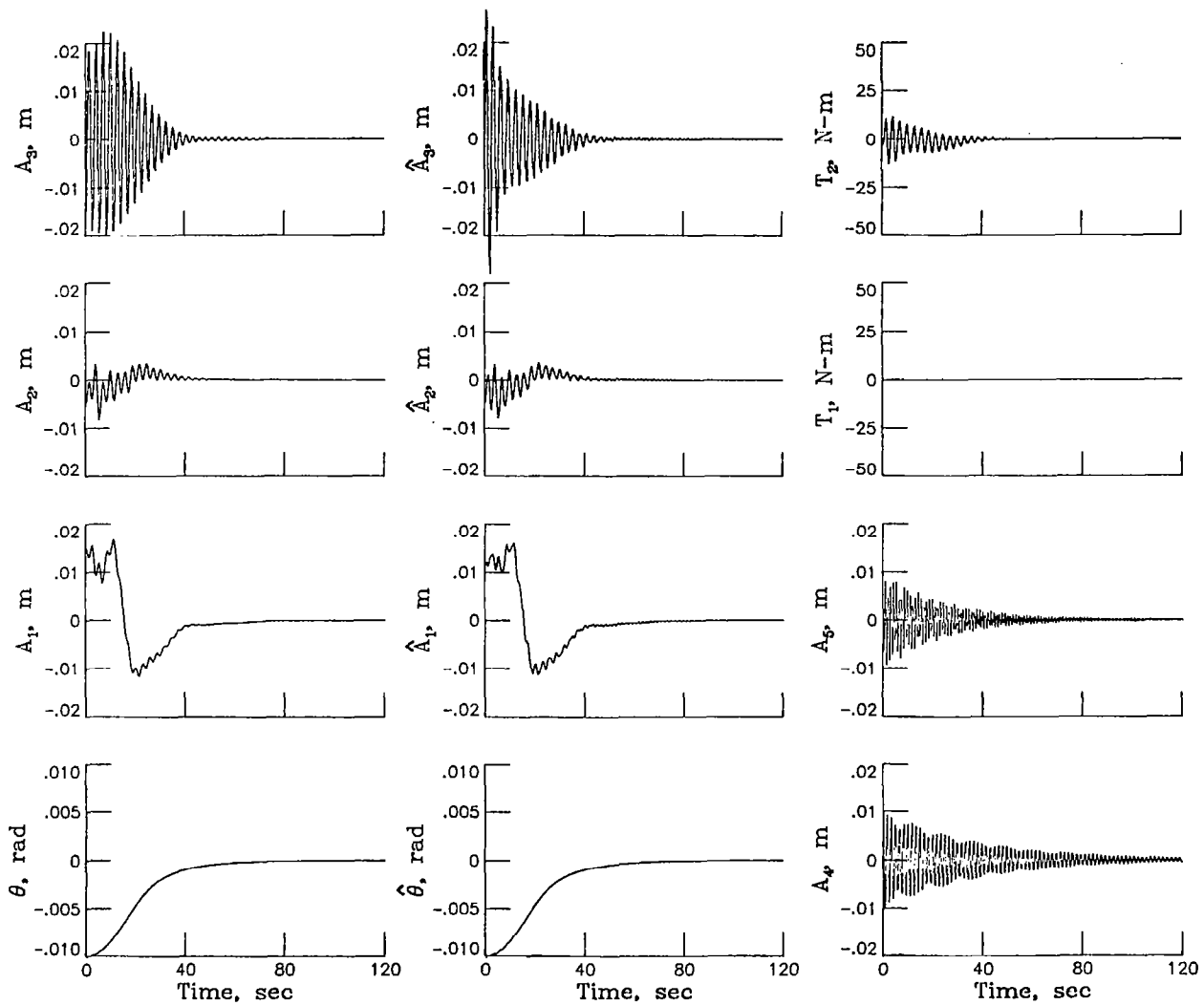
Figure 15

TWO ZERO-COMMAND PROCEDURE

The following four figures demonstrate a practical procedure for nulling
initial disturbances with two separate zero-commands. Figure 16 represents the
first zero-command and differs from the one in figure 6 in that actuator lag
(tau = 5 sec) is included and the closed-loop pitch frequency has been doubled.
Because of the increased pitch response, all disturbances are essentially nulled
within 30 seconds. The control actuators are then turned off (observer remains
on) at this time as shown in the next figure.
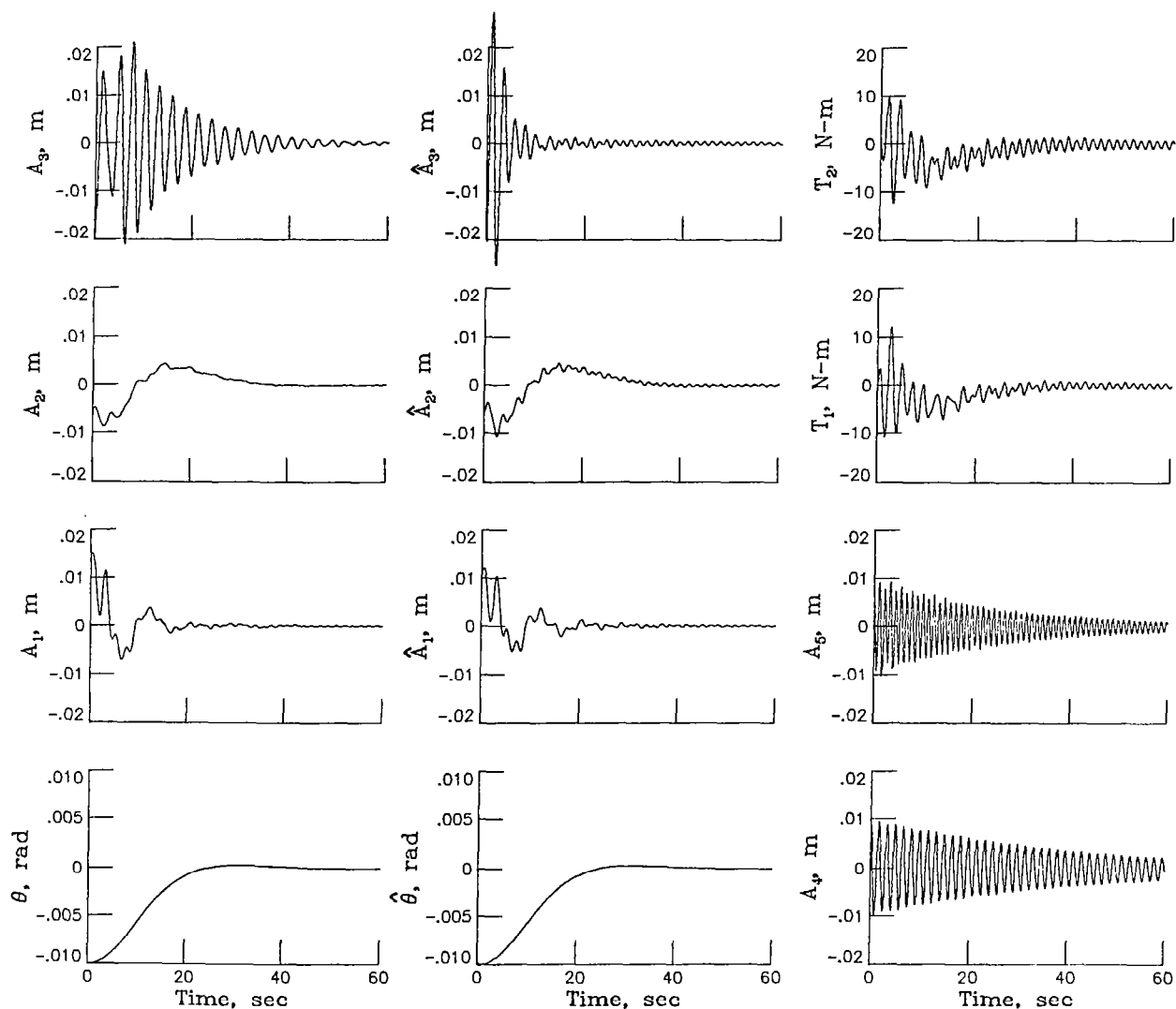
Figure 16

The results of turning off the controls at time 30 seconds are shown in figure 17. The actuators were turned off in order to avoid the oscillating control torques which are shown to persist over a long time period in figure 16. As shown in figure 17, the disturbances have not been completely nulled, but fairly good estimates of these disturbances are obtained after 30 more seconds. (Note that without the controls operating the observer is able to obtain a good estimate of A_3.) The next step, then, is to apply the second zero command at this time. The resulting responses are shown in the next figure.
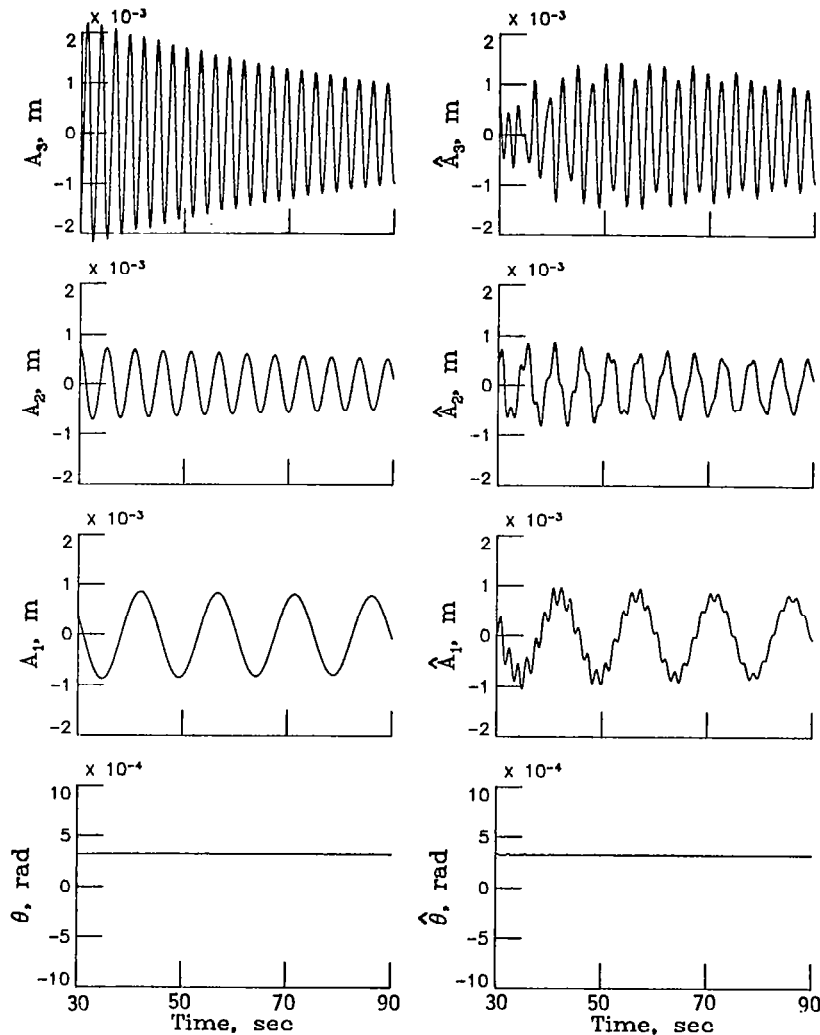
Figure 17

The modal responses in figure 18 are essentially nulled after 30 seconds. Here, the control actuators are turned off for the final time, again to avoid the oscillating control torques which would be required over a long time period. The final results of the two-zero command procedure are shown in the next figure.
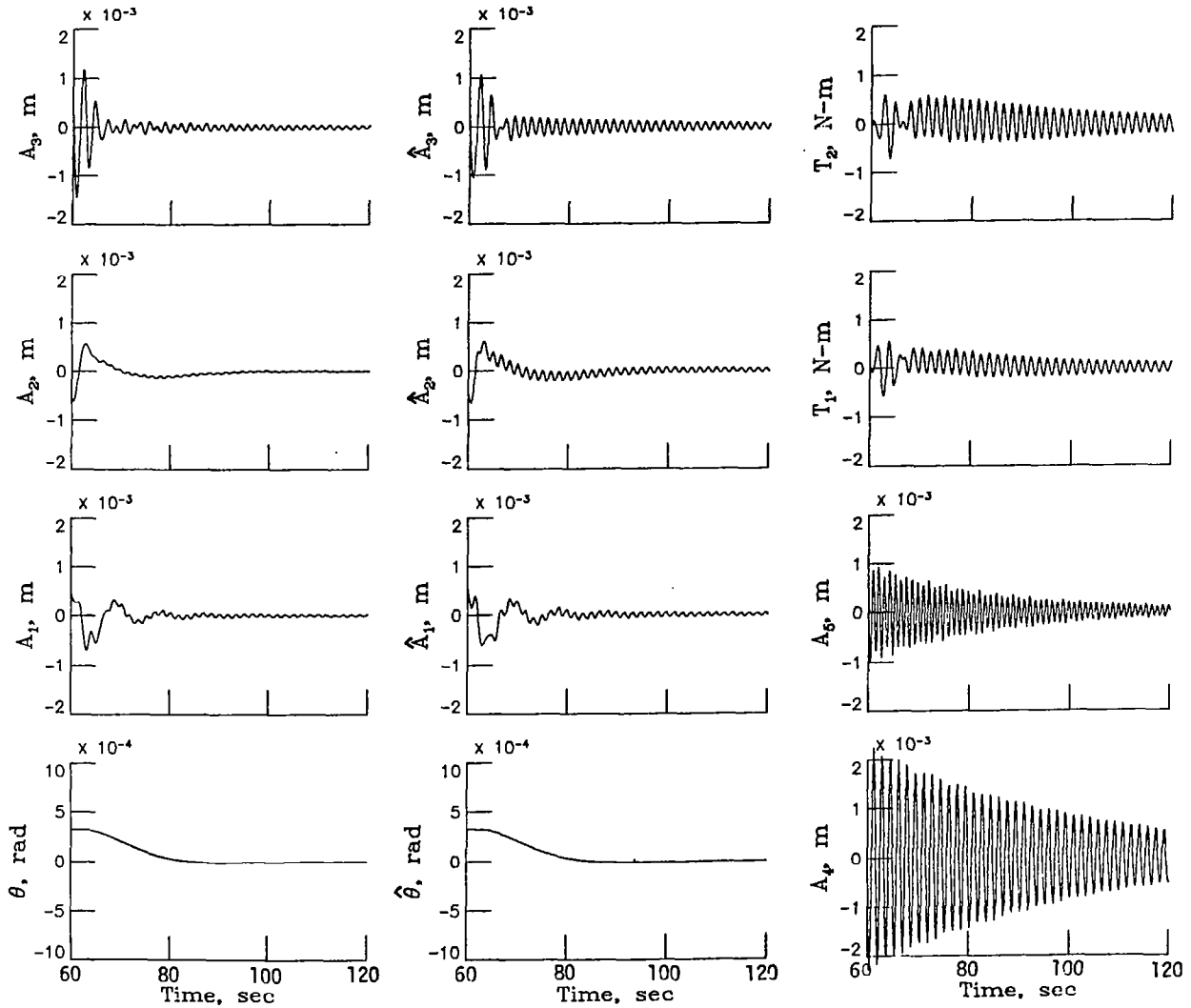
Figure 18

The results of turning off the actuators after the second zero command are shown in figure 19. The remaining disturbances are practically zero and will eventually die out through natural damping.
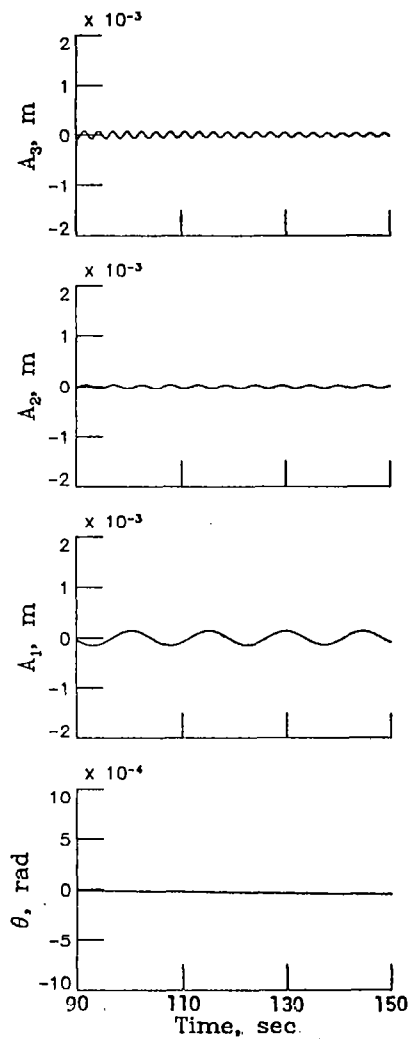
Figure 19

PITCH COMMAND - NO DISTURBANCES

   The next two figures illustrate examples of pitch commands whereby a pitch attitude of 0.01 radian is commanded. For the case in figure 20, there are no initial dusturbances, and hence no errors in the initial estimates. The commanded pitch attitude is reached in about 40 seconds, with only a small coupling effect on the second flexible mode.
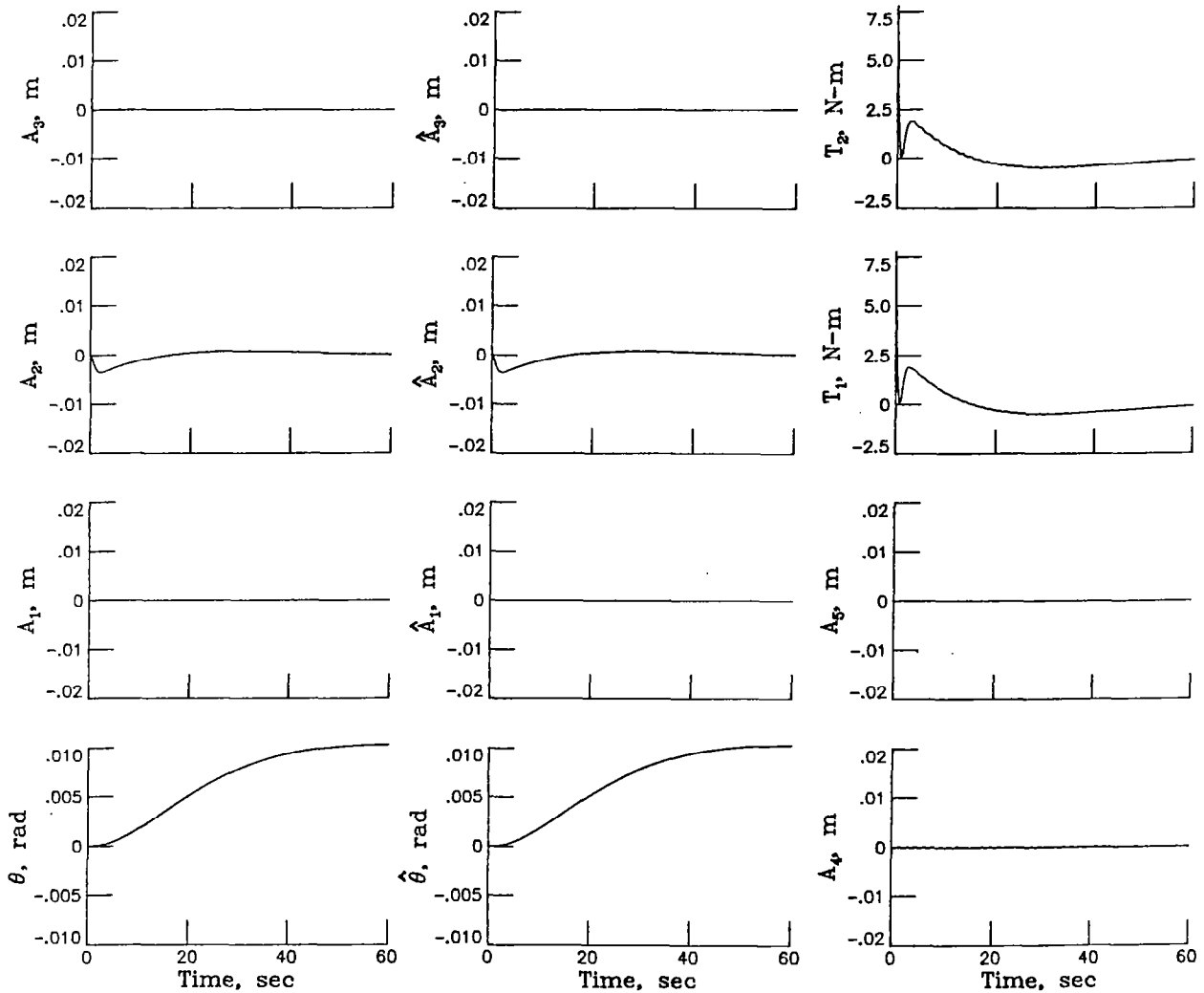
Figure 20

For the pitch command in figure 21, there is an initial pitch disturbance of -0.005 radian which is known only to an accuracy of 90 percent. The results illustrate the large effect of the initial estimate on the three modeled flexible modes. Also, the control-torque requirements are substantially increased over those of the previous figure. Doubling the error in the initial estimate would double the magnitude of these effects.
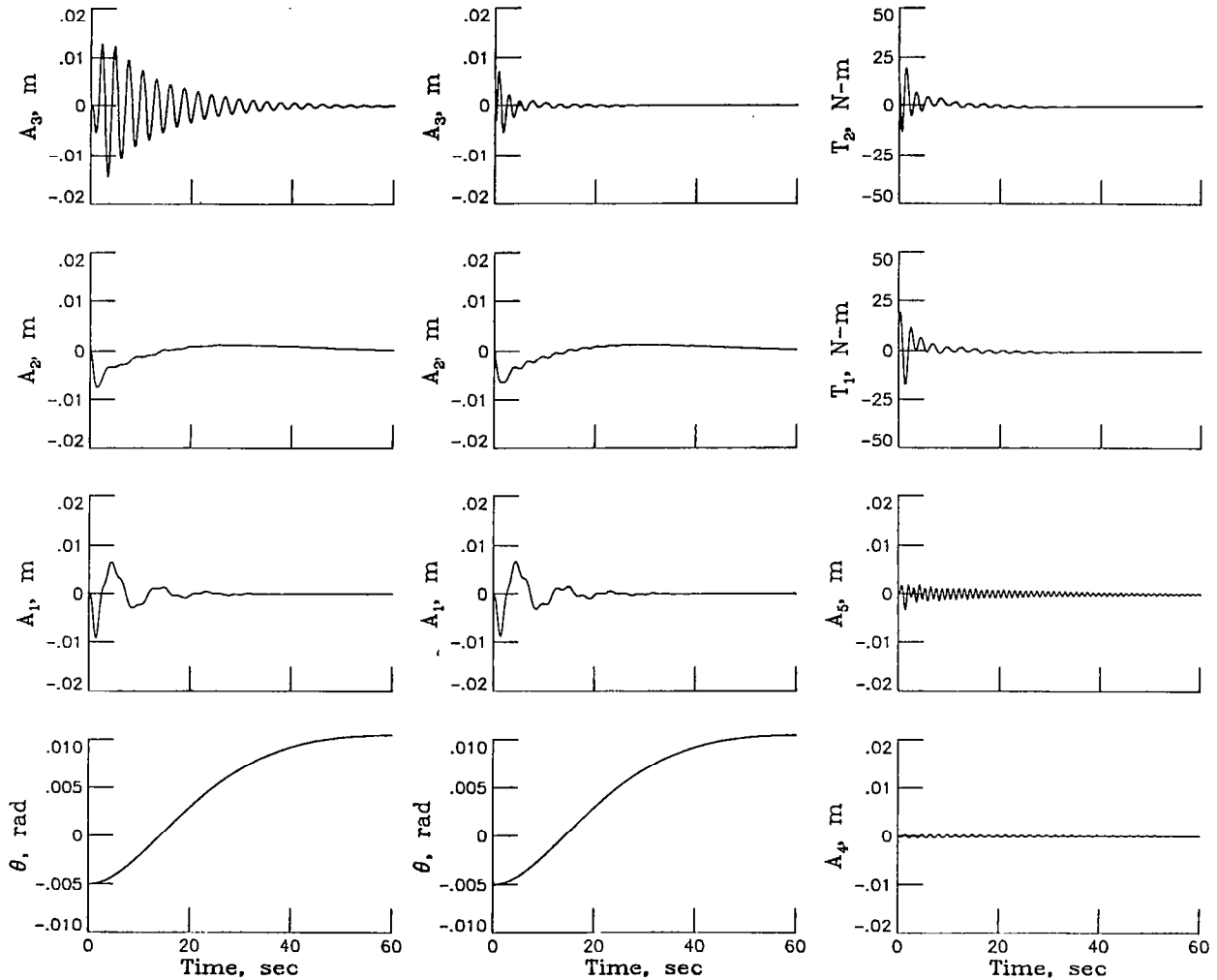
Figure 21

CONTROL REQUIREMENTS

Figure 22 compares the maximum peak actuator torques (absolute values) required for pitch and zero commands, assuming no lag in the system. The data apply to a four-actuator control system but are representative of any control arrangement. For the pitch-command data, there is an initial disturbance of -0.005 radian and the commanded value is 0.01 radian. The zero-command data pertain only to nulling initial disturbance in the flexible modes; i.e., no pitch disturbance. Except where noted, the peak torques occurred after the initial time.

As would be expected, the control requirements are essentially linearly related to the initial estimate. Also, the pitch commands require the higher control torques. Further, the results show that the requirements for zero commands increase as the accuracy of the initial estimate increase, while the opposite is true for pitch commands.
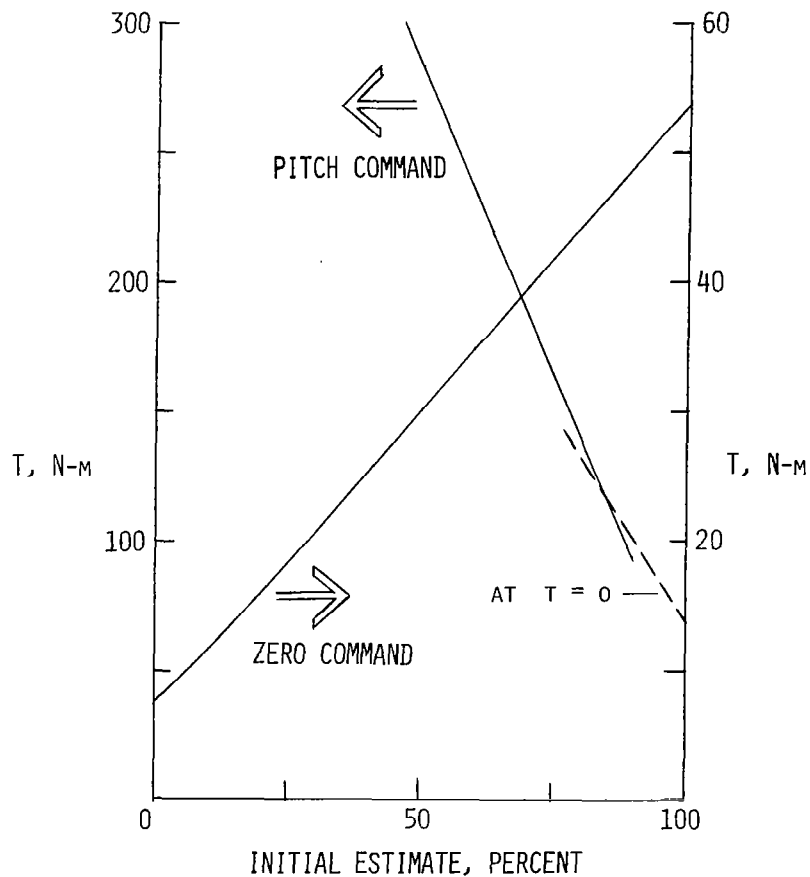
Figure 22

Figure 23 is similar to the zero command shown in figure 6, except for sensor-location error; i.e., the attitude sensors have been placed at locations other than those (nominal) used for the observer in calculating the Kalman gains. In this case the sensor locations have been moved 22.5 meters (5 percent of beam length), both in the same direction from nominal. Comparison with figure 6 shows that, except for A_5, this error produced negligible effects on system performance.
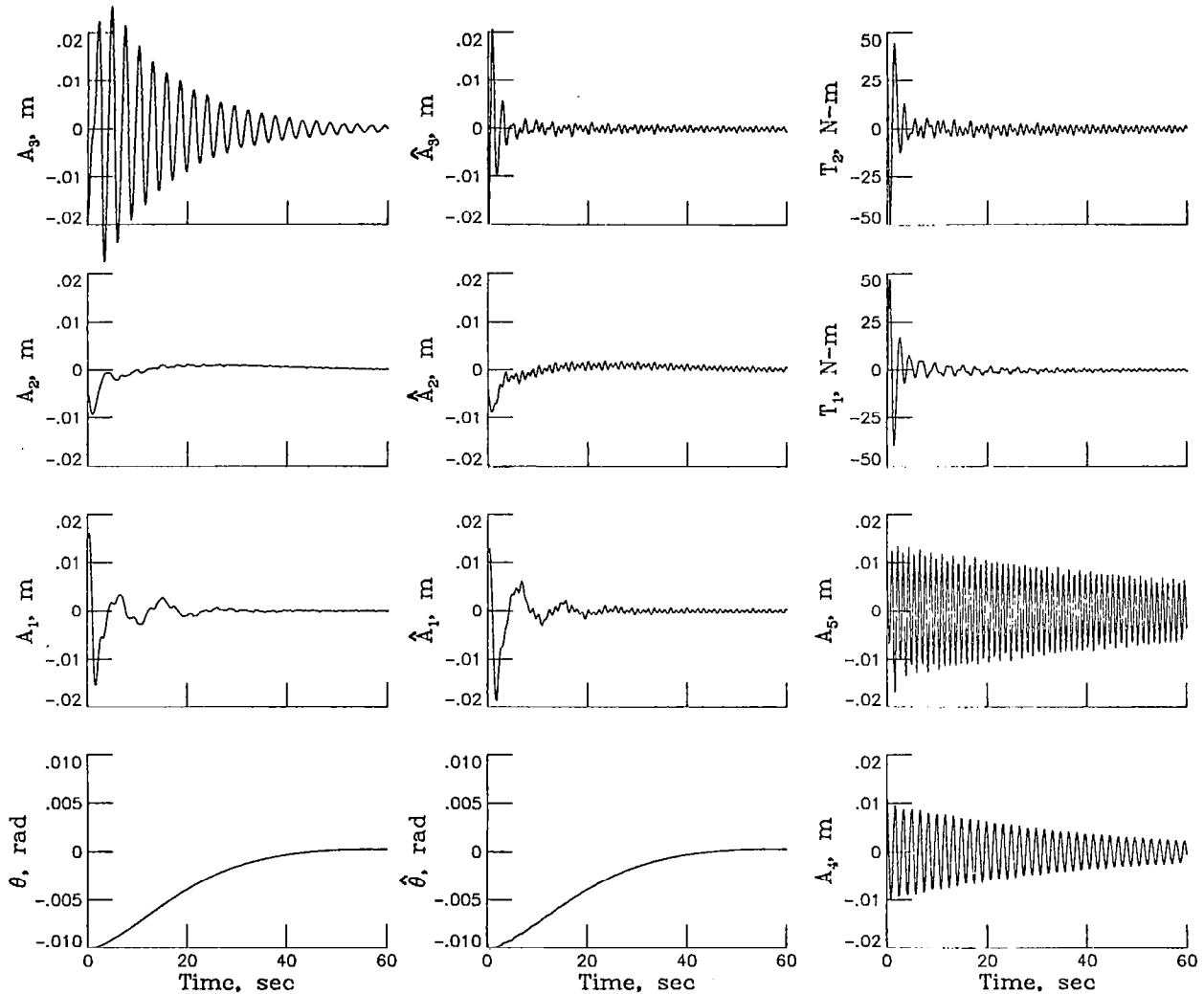

Figure 23

The case in figure 24 is the same as that for the previous figure, except the two sensors are moved in opposite directions, where the mode-slope differences from nominal (for example, sign changes) are more pronounced. Even though the system is eventually nulled, the performance is decreased as evidenced by the increased oscillations in A_3 and in the control actuators. These results can be attributed to the poor estimates in the three modeled flexible modes.
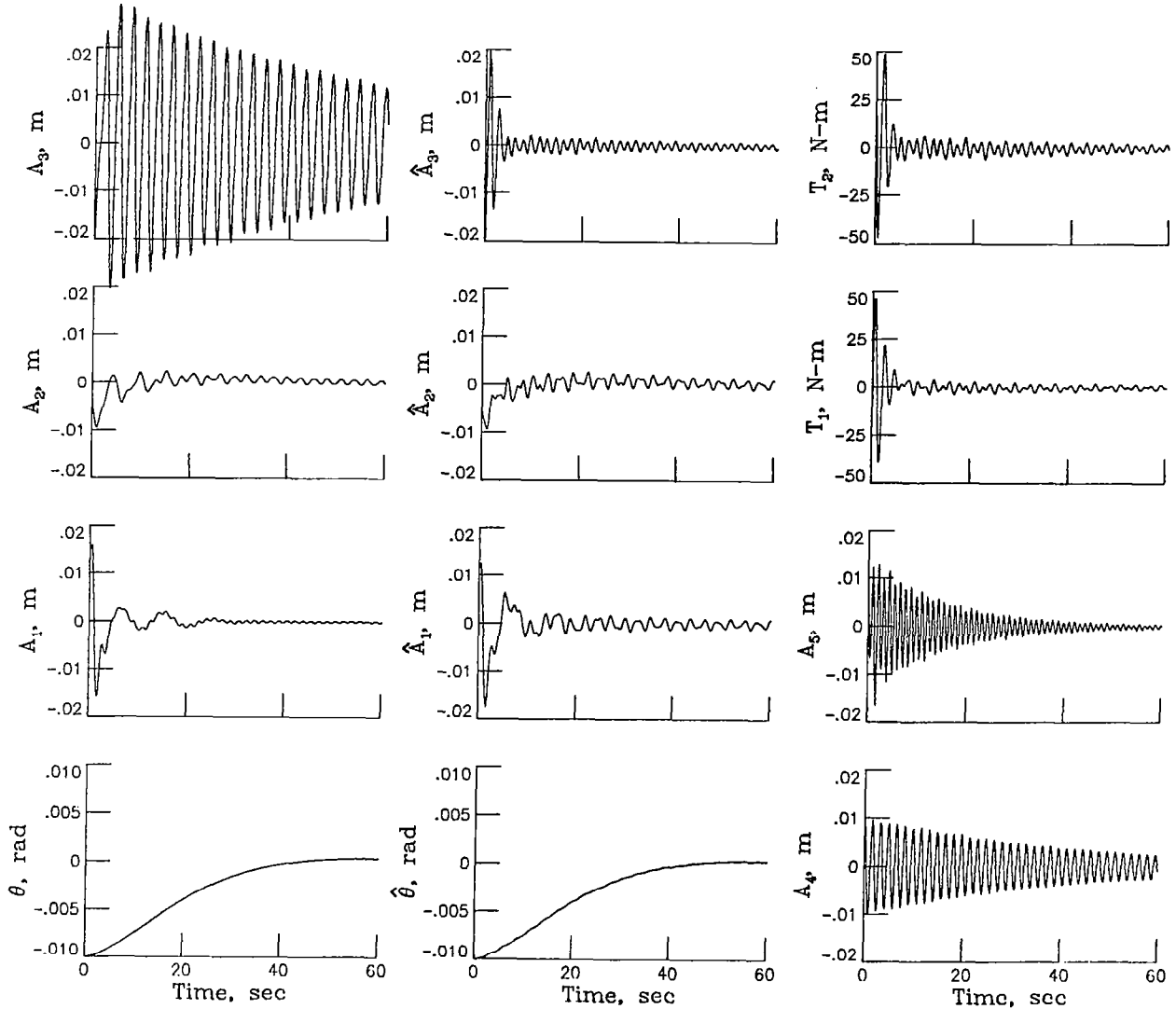
Figure 24

Relocation of the sensors 10 percent off the nominal position and in opposite directions leads to instability; this may be seen in figure 25.
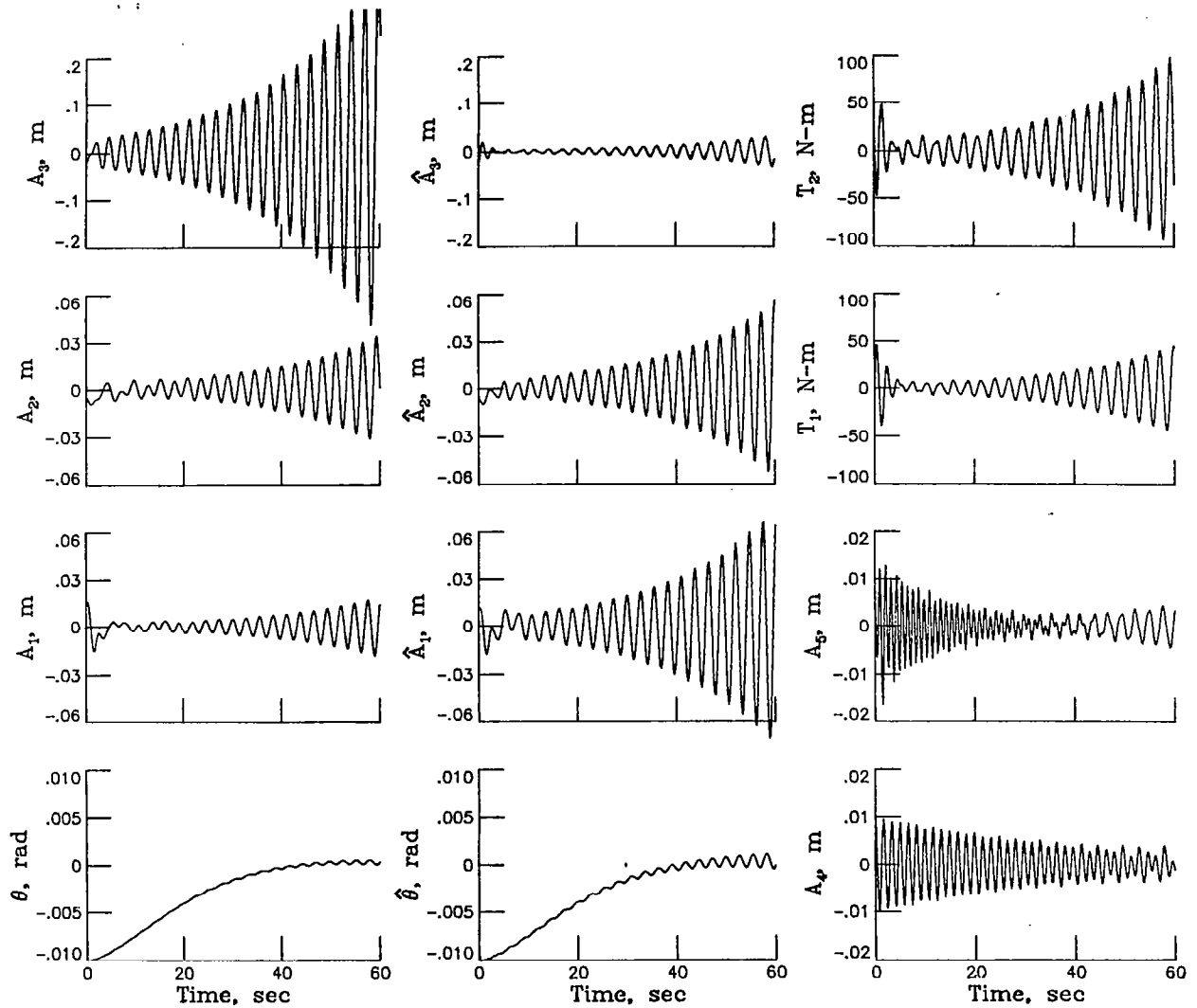

Figure 25